Unclassified

SECURITY CLASSIFICATION OF THIS PAGE (When Data Entered)

AD A042470

REPORT DOCUMENTATION PAGE

READ INSTRUCTIONS BEFORE COMPLETING FORM

1. REPORT NUMBER

2. GOVT ACCESSION NO.

3. RECIPIENT'S CATALOG NUMBER

4. TITLE (and Subtitle)
An Oceanic Mixed Layer Model Capable of Simulating Cyclic States

5. TYPE OF REPORT & PERIOD COVERED
Reprint

6. PERFORMING ORG. REPORT NUMBER

7. AUTHOR(s)
Roland W. Garwood, Jr.

8. CONTRACT OR GRANT NUMBER(s)
N0001477WR70024

9. PERFORMING ORGANIZATION NAME AND ADDRESS
Naval Postgraduate School
Monterey, CA 93940

10. PROGRAM ELEMENT, PROJECT, TASK AREA & WORK UNIT NUMBERS
NR083-275

11. CONTROLLING OFFICE NAME AND ADDRESS
Chief of Naval Research
Code 481
Arlington, VA 22217

12. REPORT DATE
24 September 1976

13. NUMBER OF PAGES
14

14. MONITORING AGENCY NAME & ADDRESS (if different from Controlling Office)
15p.

15. SECURITY CLASS. (of this report)
Unclassified

15a. DECLASSIFICATION/DOWNGRADING SCHEDULE

16. DISTRIBUTION STATEMENT (of this Report)
Approved for public release; distribution unlimited

DDC
AUG 4 1977
C

17. DISTRIBUTION STATEMENT (of the abstract entered in Block 20, if different from Report)

18. SUPPLEMENTARY NOTES
Published in Journal of Physical Oceanography, Vol. 7, No. 3, 455-468.
May 77

19. KEY WORDS (Continue on reverse side if necessary and identify by block number)
Mixed layer model
Climatological cycles
Diurnal cycle
Turbulence closure

20. ABSTRACT

A new one-dimensional bulk model of the mixed layer of the upper ocean is presented. An entrainment hypothesis dependent upon the relative distribution of turbulent energy between horizontal and vertical components is offered as a plausible mechanism for governing both entrainment and layer retreat.

This model has two properties not previously demonstrated:

(i) The fraction of wind-generated turbulent kinetic energy partitioned to potential energy increase by means of mixed layer deepening is dependent upon layer stability, $H^* = h/L$, as measured by the ratio of mixed layer depth h to Obukhov length L. This results in a modulation of the mean entrainment rate by the diurnal heating and cooling cycle.

(ii) Viscous dissipation is enhanced for increased values of $Ro^{-1} = hf/u_*$, where f is the Coriolis parameter and u_* the friction velocity for the water. This enables a cyclical steady state to occur over an annual period by limiting maximum layer depth.

A nondimensional framework used to present the general solution also suggests a basis for model comparison and data analysis.

DD FORM 1 JAN 73 1473 EDITION OF 1 NOV 65 IS OBSOLETE
S/N 0102-014-6601 |

SECURITY CLASSIFICATION OF THIS PAGE (When Data Entered)

AD No. 1
DDC FILE COPY

251 450

DISCLAIMER NOTICE

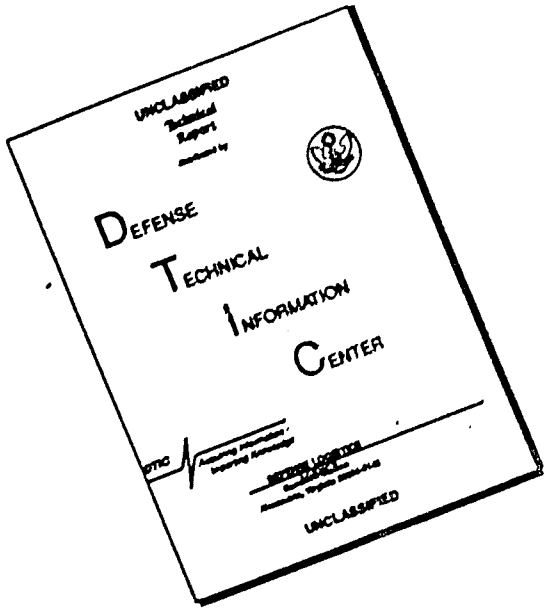

THIS DOCUMENT IS BEST QUALITY AVAILABLE. THE COPY FURNISHED TO DTIC CONTAINED A SIGNIFICANT NUMBER OF PAGES WHICH DO NOT REPRODUCE LEGIBLY.

Reprinted from JOURNAL OF PHYSICAL OCEANOGRAPHY, Vol. 7, No. 3, May 1977
American Meteorological Society
Printed in U. S. A.

An Oceanic Mixed Layer Model Capable of Simulating Cyclic States

ROLAND W. GARWOOD, JR.[1]

Department of Oceanography, Naval Postgraduate School, Monterey, Calif. 93940

(Manuscript received 24 September 1976, in revised form 14 January 1977)

ABSTRACT

A new one-dimensional bulk model of the mixed layer of the upper ocean is presented. An entrainment hypothesis dependent upon the relative distribution of turbulent energy between horizontal and vertical components is offered as a plausible mechanism for governing both entrainment and layer retreat.

This model has two properties not previously demonstrated:

(i) The fraction of wind-generated turbulent kinetic energy partitioned to potential energy increase by means of mixed layer deepening is dependent upon layer stability, $H^* = h/L$, as measured by the ratio of mixed layer depth h to Obukhov length L. This results in a modulation of the mean entrainment rate by the diurnal heating and cooling cycle.

(ii) Viscous dissipation is enhanced for increased values of $\mathrm{Ro}^{-1} = hf/u_*$, where f is the Coriolis parameter and u_* the friction velocity for the water. This enables a cyclical steady state to occur over an annual period by limiting maximum layer depth.

A nondimensional framework used to present the general solution also suggests a basis for model comparison and data analysis.

1. Introduction

The ocean mixed layer treated here is that fully turbulent region of the upper ocean that is bounded above by the sea-air interface. The wind and intermittent upward surface buoyancy flux through the surface are the sources of mechanical energy for the generation of this turbulence. Typically, the mixed layer is bounded below by a dynamically stable watermass. The vertical fluxes of heat, salt and momentum in the turbulent boundary layer or mixed layer are essentially decoupled from those of the underlying stable water column because the energy for this mixing comes from above. Minimal vertical fluxes below the mixed layer, together with high turbulence intensity within the layer, result in an approximate vertical uniformity in mean velocity and density. This ostensible homogeneity is the root of the term "slab," which is often used to describe the layer as depicted in Fig. 1. There is an appealing practical aspect to the judicious use of the assumption of vertical homogeneity in a bulk model such as this because the problem of solving for the interior fluxes of buoyancy and momentum is reduced to the need to know only the surface and entrainment fluxes. However, only small vertical gradients in these mean variables may be associated with large turbulent fluxes. Therefore the slab assumption should not be as readily applied to the turbulent kinetic energy budget.

Earlier works of concern here are those dealing explicitly with equations for the production, alteration and destruction of turbulent kinetic energy within the mixed layer. Kraus and Turner (1967) were the first to heed the turbulent kinetic energy budget in the prototype one-dimensional mixed layer model, utilizing the approximately decoupled state of the equations for the thermal and mechanical energies. By neglecting the frictional generation of heat, the vertically integrated heat equation provides a relationship for the conservation of potential energy. However, viscous dissipation cannot be neglected in the turbulent kinetic energy budget. This last aspect has been recognized only more recently. Dissipation has been assumed to be a fixed fraction of wind stress production in the models of Geisler and Kraus (1969), Miropol'skiy (1970), Denman (1973) and Niiler (1975), all variations of the Kraus-Turner model. The latest parameterizations of dissipation, those by Elsberry *et al.* (1976), Resnyanskiy (1975) and Kim (1976), have been conceived with the recognition of a need to augment dissipation in certain instances.

These earlier theories that are based on the turbulent energy equation demonstrate the importance of the Obukhov length scale L [as first applied to the ocean by Kitaigorodsky (1960)]. However, they have not explained the significance of another length scale,

[1] The author was supported during this research at the University of Washington, Seattle, by NOAA's Environmental Research Laboratories and by NOAA's GATE Office.

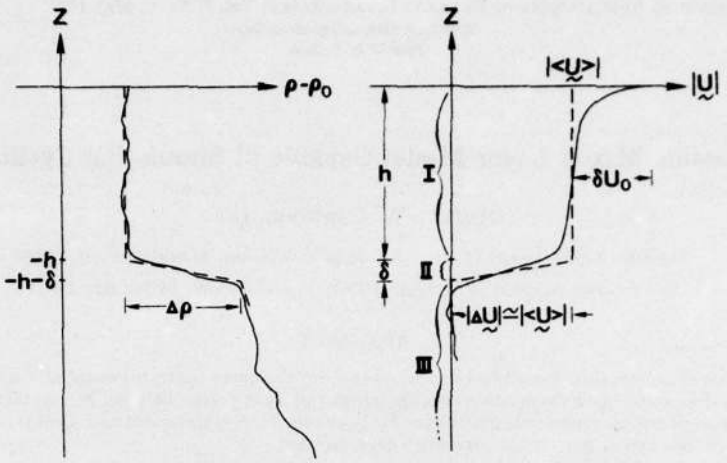

FIG. 1. Idealized density and mean velocity profiles of the ocean mixed layer. Region I is the fully-turbulent ($Rf<Rf_{cr}$) mixed layer of depth h. Region II is the slightly stable ($Rf=R\delta\sim 1$), intermittently-turbulent entrainment zone of thickness δ. Region III is the stable ($Ri>Ri_{cr}$) underlying watermass having negligible vertical fluxes in comparison to those of region I. Rf and Ri are the flux and gradient Richardson numbers, respectively.

u_*/f, as proposed by Rossby and Montgomery (1935). Specifically, the general applicability of these models is limited by the following three problems:

1) Gill and Turner have demonstrated the inability of the prototype model to predict cyclical steady state on an annual basis. If the viscous dissipation of turbulent energy is parameterized as a fixed fraction of production, the fraction of wind-generated energy going to entrainment mixing is constrained to be constant by the integral relationship, regardless of the layer depth. Testing such a model Camp (1976) shows that the predicted deepening during storms is much too rapid and unchecked. An enhancement of dissipation is one possible answer, but a physical explanation is required. In a departure from the Kraus-Turner approach, Pollard *et al.* (1973) used the *total* kinetic energy equation in a model which postulates a mean flow instability as the mechanism for deepening. Most recent efforts, however, have involved modeling of the terms of the turbulent part of the kinetic energy budget. It is recognized here that the Pollard *et al.* model does predict a possible cyclical steady state. However, their model fails to consider the turbulence generated *above* the entrainment zone as a source of energy for mixing *within* the zone. A mean flow instability does not seem to be the dominant mechanism for significant layer deepening, and simulations using this model fall short of predicting the observed amount of deepening.

2) The stable regime ($H^*>0$) for the turbulent boundary layer is not well understood, especially in the limiting case of retreat, i.e., $\partial h/\partial t\leqslant 0$. Retreat occurs when the *vertical* component of turbulence is insufficient to transport heat, momentum and turbulence to an earlier-established depth of mixing. Knowledge of the distribution of turbulent energy between horizontal and vertical components is therefore crucial in predicting cessation of mixing, i.e., layer retreat. The earlier users of an equation for the *total* turbulent energy have neglected this distributional factor.

3) In most previous models, all buoyant production of turbulent energy has been consigned to potential energy increase, or $r=1$, where r is the ratio of downward entrainment buoyancy flux to upward surface buoyancy flux, $-\overline{bw}(-h)/\overline{bw}(0)$. This could only be possible if none of the convectively-produced turbulent energy were dissipated. Numerous[2] measurements show that r is much less than unity. This problem is not solved by taking dissipation to be a fixed fraction of shear production plus buoyant production (less buoyant damping) because layer retreat will then be predicted only if buoyant damping equals shear production, making the value assigned to dissipation be equal to zero. However, if there is turbulence available for buoyancy flux, there must also be dissipation. Both this apparent dilemma and the retreat problem are part of a single larger problem: $\partial h/\partial t$ should not be the direct consequence of an integral constraint on the total turbulent energy equation.

In an attempt to resolve the above three problems, this paper offers a new one-dimensional model of the mixed layer in which several processes are parameterized more explicitly than in previous models. First, the fraction of wind-generated turbulent kinetic energy available for mixing is dependent on the ratio of the mixed layer depth to the Obukhov mixing length.

[2] Stull (1975) lists experimental observations of r (his A_1), and the median value is between 0.1 and 0.3.

Second, viscous dissipation is dependent on a local Rossby number. Third, separate vertical and horizontal equations for turbulent kinetic energy are used, allowing for a more explicit treatment of the mixing process.

Mean turbulent field modeling of the terms of these component equations is necessary to put the model in closed form. There is no particular precedent for doing this in a bulk model, but Bradshaw (1972), Mellor and Herring (1973) and Lumley and Khajeh-Nouri (1974) provide a general background for the technique.

In the model to be presented here, conservation of buoyancy is employed as a generalization of the conservation of heat alone. The buoyancy equation is generated from the heat and salt equations together with an equation of state,

$$\tilde{\rho}=\rho_0[1-\alpha(\tilde{\theta}-\theta_0)+\beta(\tilde{s}-s_0)], \tag{1}$$

and the definition for buoyancy,

$$\tilde{b}=g(\rho_0-\tilde{\rho})/\rho_0. \tag{2}$$

In (1) and (2) $\tilde{\theta}$ is temperature, $\tilde{s}$ salinity and $\tilde{\rho}$ density, while α and β are the expansion coefficients for heat and salt, respectively, and g is gravity. The tilde represents the total instantaneous value and the subscript zero denotes a representative but arbitrary value. The generalization of using $\tilde{b}$ rather than $\tilde{\theta}$ will cast the model equations in a form equally applicable to those situations where evaporation and precipitation contribute significantly to the surface buoyancy flux and the structure of the evolving pycnocline. The buoyancy equation also has a more obvious and direct role in the mechanical energy budget, as shown in Fig. 2.

2. Entrainment

a. Conceptual model

A physically plausible and accurate model for predicting the rate of deepening (or retreat) is dependent upon an understanding of the dynamics of the entrainment process. The assumption is that the turbulence of the overlying mixed layer provides the energy needed to destabilize and erode the underlying stable water mass. Therefore the turbulent kinetic energy budget is the basis for the entrainment

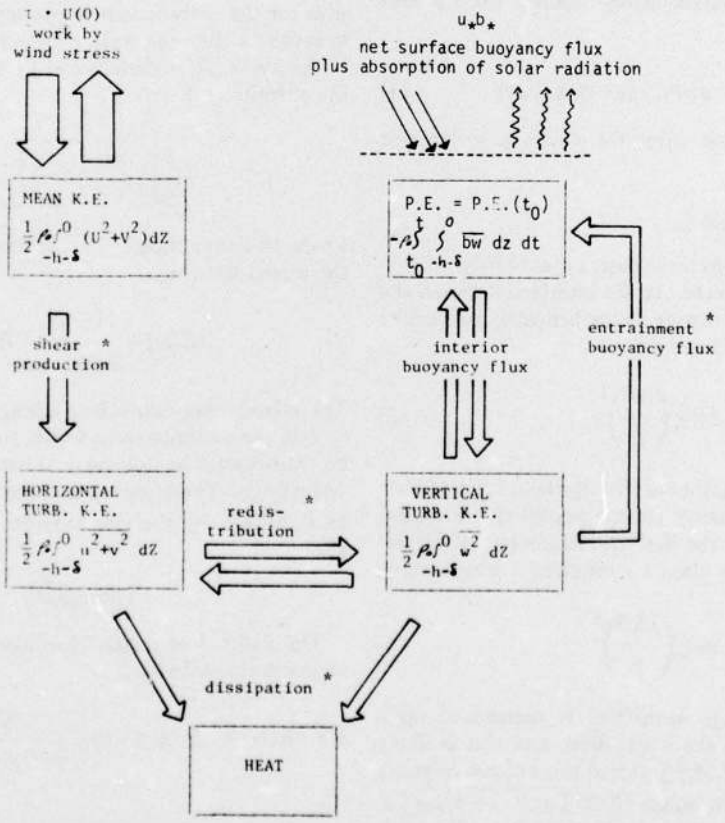

FIG. 2. Mechanical energy budget for the ocean mixed layer. Asterisks indicate those processes that must be parameterized to close the system of equations.

hypothesis:

$$\frac{1}{2}\frac{\partial(\overline{u^2}+\overline{v^2}+\overline{w^2})}{\partial t}=-\left[\overline{uw}\frac{\partial U}{\partial z}+\overline{vw}\frac{\partial V}{\partial z}\right]+\overline{bw}-\frac{\partial}{\partial z}\left[\overline{w\left(\frac{u^2+v^2+w^2}{2}+\frac{p}{\rho_0}\right)}\right]-\epsilon\approx 0, \quad (3)$$

where ϵ is viscous dissipation and ensemble mean and fluctuating components are denoted by the upper and lower cases respectively. For example, $\tilde{u}=U(z,t)+u(x,y,z,t)$, where $U=\bar{\tilde{u}}$. If the terms of (3) are known throughout the boundary layer then the evolution of the potential energy and density profile may be evaluated by using the budget for mechanical energy.

In the conceptual model, the entrainment zone (region II of Fig. 1) is a region which is intermittently turbulent in comparison with the overlying region I. Local turbulent intensity and the work rate by this turbulence on the interface ($z=-h$) in the form of $-\overline{bw}(-h)$ is dependent upon the rate of supply of energy from above, $-(\partial/\partial z)[\overline{w(E/2+p/\rho_0)}]_{-h}$, where $E=u^2+v^2+w^2$. Without this extra energy source, the region will remain dynamically stable, with a flux Richardson number

$$\mathrm{Rf}=\overline{bw}/(\overline{uw}\partial U/\partial z+\overline{vw}\partial V/\partial z) \quad (4)$$

larger than the critical value for a return to laminar flow.

b. The specific mechanism

Of Benjamin's (1963) three basic types of instabilities, two may be possible here. At the interface between the mixed layer and the denser water beneath, a so-called class A instability will arise if

$$\Delta\tilde{u}\gtrsim\left(\frac{\Delta B}{k}\right)^{\frac{1}{2}}, \quad (5)$$

where k is the wavenumber of the interfacial disturbance and $\Delta\tilde{u}$ the total velocity change across the interface. From Lamb (1932), the Kelvin-Helmholtz (K-H) instability (Benjamin's class C) requires a larger value for $\Delta\tilde{u}$:

$$\Delta\tilde{u}\gtrsim\left(\frac{2\Delta B}{k}\right)^{\frac{1}{2}}. \quad (6)$$

However, the class A instability is dependent upon energy dissipation in the lower fluid, and this is likely to be small compared with inferred rates of convergence of energy flux at the interface $(\partial/\partial z)[\overline{w(E/2+p/\rho_0)}]_{-h}$. For geophysical flows of this type having large Reynolds and Péclet numbers, the class C instability is therefore most likely to be the dominant mechanism leading to observed rates of entrainment.

The specific mechanism that is envisioned in the destabilization of the interface and the resulting entrainment is a "local" K-H instability. The onset of this instability and its exponential growth rate is predicted by linear two-dimensional wave theory. As individual wave packets achieve a significant amplitude, the nonlinear three-dimensional effects of the turbulence field are assumed to prevail and to advect parts of the exposed cusps of denser water up into the mixed layer. Therefore, it is only the initial stages of the instability that are strictly of the K-H type, where the induced suction at the crests of a perturbation wave on the interface is large enough to overcome the restoring buoyancy force. The shear needed to trigger such an instability is provided by the local turbulent eddies. The mean shear contributes to the instability but usually cannot in itself generate a critical Richardson number or directly influence the frequency and magnitude of the destabilizing events.

c. Entrainment hypothesis derived

Since the presumption is that the convergence of flux of turbulent energy at the interface is primarily responsible for the entrainment buoyancy flux, the problem is to estimate the time scale τ_e required to transport some of the available turbulent energy $\langle\bar{E}\rangle$ to the vicinity of the entraining interface:

$$-\frac{\partial}{\partial z}\left[\overline{w\left(\frac{E}{2}+\frac{p}{\rho_0}\right)}\right]_{-h}=\frac{\langle\bar{E}\rangle}{\tau_e}, \quad (7)$$

where the angle braces denote the vertical mean over the mixed layer, i.e.,

$$\langle\bar{E}(t)\rangle=\frac{1}{h+\delta}\int_{-h-\delta}^{0}\bar{E}(z,t)dz. \quad (8)$$

The mixed layer depth h or a length scale proportional to h is the distance over which turbulent energy must be transported by the vertical component of turbulent velocity w. Therefore τ_e is taken to be proportional to h divided by the rms vertical velocity scale, $\langle\overline{w^2}\rangle^{\frac{1}{2}}$, giving

$$\tau_e=a_1h\langle\overline{w^2}\rangle^{-\frac{1}{2}}. \quad (9)$$

The width δ of region II is assumed to adjust so as to maintain stability:

$$\mathrm{R}\delta=\mathrm{Rf}(-h-\delta<z<-h)\approx\frac{\delta\Delta B}{(\Delta U)^2+(\Delta V)^2}=\text{constant}, \quad (10)$$

where Δ denotes the drop in the mean variable across

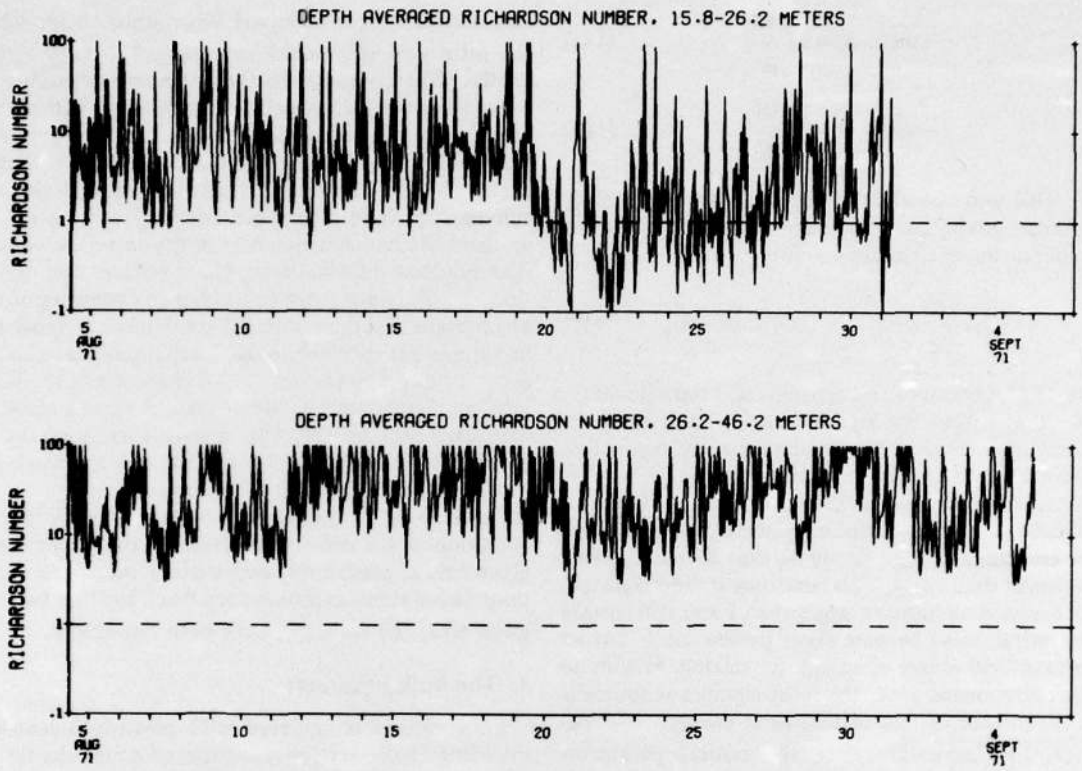

FIG. 3. From Halpern (1974) showing a storm on 20 August that deepened the mixed layer to about 24 m.

the interface. A too-sharp interface ($\delta\sim 0$) would be dynamically unstable for all wavenumbers ($k\lesssim\delta^{-1}$) with any finite mean velocity drop $|\Delta U_i|$. The resultant vertical mixing would increase δ until (10) was satisfied. On the other hand, interfacial instabilities and subsequent mixing will sharpen ($\delta\to 0$) the interface, explaining the very sharp interfaces observed in grid-stirred experiments where $\Delta U_i\sim 0$. The combined effect of these two tendencies is to maintain an equilibrium value for δ so that Rδ remains constant. It is important to realize here that the assumption that $R\delta$ is constant does not constitute closure because the value of δ is not a known quantity. This concept of the interface dynamics and the role of Rδ follows closely the argument of Csanady (1974). The closure hypothesis of Pollard *et al.*, (1973), $h\Delta B/(\Delta U^2+\Delta V^2)=$ constant, is derived from (10) only by making the additional assumption that $h/\delta=$ constant. However, the entrainment with shear by Moore and Long (1971) supports (10) and indicates that h/δ is not constant. Halpern's (1974) measurements of depth-averaged gradient Richardson number versus time (Fig. 3) also lend support to (10). As the vertical position of the interface was modulated by tidal-frequency internal waves, the position of the current meters may have passed into or through the interface region, depending upon both the average mixed-layer depth and the amplitude of the internal wave. The storm on 20 August deepened the layer sufficiently to influence the envelope for 15.8–26.2 m but not for 26.2–46.2 m.

With Fig. 1 in mind, Rf may be expressed in terms of the bulk model properties by integrating the mean buoyancy and momentum equations

$$\frac{\partial B}{\partial t}=-\frac{\partial\overline{bw}}{\partial z}+\frac{\alpha g}{\rho_0 C_p}Q, \tag{11}$$

$$\frac{\partial U}{\partial t}=fV-\frac{\partial\overline{uw}}{\partial z}, \tag{12a}$$

$$\frac{\partial V}{\partial t}=-fU-\frac{\partial\overline{vw}}{\partial z}, \tag{12b}$$

across the entrainment zone, from $z=-h-\delta$ to $z=-h$. If negligible amounts of momentum and buoyancy are transported below the entrainment zone, and the interface doesn't change significantly, then this integration yields the so-called jump conditions for turbulent fluxes at the bottom of the mixed layer:

$$-\overline{bw}(-h)=\Delta B\frac{\partial h}{\partial t}, \tag{13}$$

$$-\overline{uw}(-h)=\Delta U\frac{\partial h}{\partial t}, \tag{14a}$$

$$-\overline{vw}(-h)=\Delta V\frac{\partial h}{\partial t}. \tag{14b}$$

Using (10) and the above jump conditions, one finds that shear production is a fixed fraction of buoyant damping in the entrainment zone:

$$-\overline{u_i w}\frac{\partial U_i}{\partial z}(-h)=-(\mathrm{R}\delta)^{-1}\overline{bw}(-h), \tag{15}$$

where $(\mathrm{R}\delta)^{-1}$ becomes the constant of proportionality. Notice that within the accuracy of (13) and (14), the flux and gradient Richardson numbers are equivalent (and equal to $\mathrm{R}\delta$) in the entrainment zone.

Tennekes (1973) assumed that dissipation is an insignificant part of the turbulent kinetic energy budget in the entrainment zone, implying that $\mathrm{R}\delta$ must have a value larger than unity. This zone may indeed maintain a flux Richardson number larger than 1 and still sustain active entrainment because shear production is not an important *local* source of energy for mixing. Within an active entrainment zone, the most significant source is the convergence of flux of turbulent energy, $-(\partial/\partial z)\times[\overline{w(E/2+p/\rho_0)}]$. Therefore the critical parameter determining the rate of entrainment is not Rf but is instead the ratio P of buoyancy flux to convergence of energy flux, i.e.,

$$P=\overline{bw}\Big/\frac{\partial}{\partial z}\left[\overline{w\left(\frac{E}{2}+\frac{p}{\rho_0}\right)}\right]. \tag{16}$$

Then (7), (9) and (16) give an entrainment equation,

$$P(-h)=h\overline{bw}(-h)/\langle\overline{w^2}\rangle^{\frac{1}{2}}\langle\bar{E}\rangle=m_4, \tag{17}$$

if $P(-h)$ is the critical constant parameter, assigned the value m_4.

If dissipation in the entrainment zone is either negligible or is a fixed fraction of the flux convergence, i.e.,

$$\epsilon(-h)=a_2\langle\bar{E}\rangle/\tau_e, \tag{18}$$

then (17) is also the consequence of (3), (7), (9), (15) and (18) where m_4 reflects the combination of the constants of proportionality:

$$m_4=\frac{(1-a_2)\mathrm{R}\delta}{a_1(\mathrm{R}\delta-1)}.$$

Eq. (17) is similar to the form in Tennekes (1973), with the primary difference being the use of $\langle\overline{w^2}\rangle^{\frac{1}{2}}\langle\bar{E}\rangle$ rather than simply $\langle\bar{E}\rangle^{\frac{1}{2}}$. This feature should generalize the applicability of the final mixed layer model, enabling its use under a wide span of conditions, i.e., the diurnal and annual ranges of mixed layer stability for which the ratio $\langle\overline{w^2}\rangle/\langle\bar{E}\rangle$ would be expected to vary significantly. This approach to the entrainment problem is very different theoretically from that of Mellor and Durbin (1975). Although both theories employ mean-turbulent-field modeling techniques in the turbulent energy budget, Mellor and Durbin neglect the flux convergence term altogether and rely upon a critical gradient Richardson number at the interface coupled with gradient diffusion *below* the interface. The derivation of (17), from Garwood (1976), is based upon the assumption that the instability mechanism is dynamical in nature, but the Mellor and Durbin parameterization depends upon the viscous ($\nu\neq 0$) character of the interface, as in Benjamin's (1963) class A type instability. Measurements of the flux convergence term at an entraining interface are nonexistent but are needed to settle this very fundamental difference.

Eq. (17) does not close the problem of predicting the evolution of the density structure of the upper ocean, given initial conditions, and surface boundary conditions (wind stress and buoyancy flux), because two new unknowns, $\langle\bar{E}\rangle$ and $\langle\overline{w^2}\rangle$, have been introduced.

3. The bulk equations

Final closure is achieved with mean-turbulent-field modeling of the vertically integrated equations for the individual turbulent kinetic energy components, plus the inclusion of the bulk buoyancy and momentum equations.

With rectangular coordinate axes having x positive to the east, y positive to the north and z positive upward, the individual turbulent kinetic energy budgets are given by

$$\frac{1}{2}\frac{\partial\overline{u^2}}{\partial t}=-\overline{uw}\frac{\partial U}{\partial z}-\frac{\partial}{\partial z}\left(\frac{\overline{wu^2}}{2}\right)+\overline{\frac{p}{\rho_0}\frac{\partial u}{\partial x}}+\Omega_3\overline{uv}-\Omega_2\overline{uw}-\epsilon/3, \tag{19a}$$

$$\frac{1}{2}\frac{\partial\overline{v^2}}{\partial t}=-\overline{vw}\frac{\partial V}{\partial z}-\frac{\partial}{\partial z}\left(\frac{\overline{wv^2}}{2}\right)+\overline{\frac{p}{\rho_0}\frac{\partial v}{\partial y}}-\Omega_3\overline{uv}-\epsilon/3, \tag{19b}$$

$$\frac{1}{2}\frac{\partial\overline{w^2}}{\partial t}=\overline{bw}-\frac{\partial}{\partial z}\left(\frac{\overline{w^3}}{2}+\overline{\frac{wp}{\rho_0}}\right)+\overline{\frac{p}{\rho_0}\frac{\partial w}{\partial z}}+\Omega_2\overline{uw}-\epsilon/3. \tag{19c}$$

In deriving these equations, horizontal homogeneity was assumed, neglecting those terms containing mean horizontal gradients. The sum of these three component equations gives (3), the *total* turbulent kinetic energy budget. Each of the component equations is usually in a quasi-steady state because the dissipation time scale is usually much smaller than the time scale of the surface fluxes. A steady-state assumption will simplify final solution, but it is not actually necessary to achieve

closure. Notice that the redistribution terms associated with rotation, $\Omega_\alpha \overline{u u_\alpha}$, and pressure interaction,

$$\overline{\frac{p}{\rho_0}\frac{\partial u_\alpha}{\partial x_\alpha}},$$

vanish in the summation. These terms therefore did not appear and therefore played no role in the earlier models in which the turbulent energy budget was not separated into components. Vertical integration of (11) and (12a,b) yields the bulk relationships for mean buoyancy

$$h\frac{\partial\langle B\rangle}{\partial t}+\Delta B\frac{\partial h}{\partial t}-\Lambda=\frac{\alpha g Q_0}{\rho_0 C_p}-\overline{bw}(0), \tag{20}$$

and mean momentum

$$h\frac{\partial\langle U\rangle}{\partial t}+\Delta U\frac{\partial h}{\partial t}-\Lambda=fh\langle V\rangle-\overline{uw}(0), \tag{21a}$$

$$h\frac{\partial\langle V\rangle}{\partial t}+\Delta V\frac{\partial h}{\partial t}-\Lambda=-fh\langle U\rangle-\overline{vw}(0). \tag{21b}$$

Three assumptions were employed in this integration:

(i) Vertical fluxes are negligible below the mixed layer. Therefore,

$$\overline{bw}(-h-\delta)=\overline{uw}(-h-\delta)=\overline{vw}(-h-\delta)=0.$$

(ii) The mixed layer is sufficiently homogeneous so that

$$\Delta B\approx\langle B\rangle-B(-h-\delta),$$
$$\Delta U\approx\langle U\rangle-U(-h-\delta),$$
$$\Delta V\approx\langle V\rangle-V(-h-\delta).$$

(iii) Horizontal homogeneity is assumed for all mean variables. The approximation of local horizontal homogeneity with regard to the mean turbulence fields is usually an accurate assumption because of the short time scale for the turbulence. On the other hand, it is recognized that the mean buoyancy and momentum fields are not one-dimensional for all time and space scales. However, such advective effects shall be neglected here in order to emphasize some new aspects which are fundamental to the one-dimensional model.

4. Closure hypotheses

Mean turbulent field modeling of the terms of (19a–c), integrated across the mixed layer, will close the problem. That is, there will be five equations for the five unknowns

$$h,\quad \langle B\rangle,\quad \langle C\rangle=\langle U\rangle+i\langle V\rangle,\quad \langle\overline{w^2}\rangle,\quad \langle\overline{u^2}+\overline{v^2}\rangle.$$

In addition, there will be empirical constants to be specified.

a. *Viscous dissipation*

For fully turbulent geophysical flows having large Reynolds numbers, viscous dissipation of the turbulence occurs primarily in the small eddies which are locally isotropic. As explained by Tennekes and Lumley (1972), an estimate of dissipation is made by taking the rate at which the largest eddies supply energy to the smaller eddies (equal to the rate of dissipation) to be proportional to the reciprocal of the time scale of the largest eddies. The net rate of dissipation,[3]

$$D=\int_{-h-\delta}^{0}\epsilon dz=\int_{-h-\delta}^{0}\nu\overline{\frac{\partial u_i}{\partial x_j}\frac{\partial u_i}{\partial x_j}}dz, \tag{22}$$

and the vertical mean of turbulent energy, $\langle E\rangle$, are accordingly used to define a dissipation time scale, $\tau_\epsilon=\langle E\rangle/\langle\epsilon\rangle$, or

$$\langle\epsilon\rangle=\frac{\langle E\rangle}{\tau_\epsilon}. \tag{23}$$

1) Dissipation in shallow mixed layers, Ro≫1

If the time scale of these largest eddies is proportional to the mixed layer depth divided by the rms turbulent velocity, i.e.,

$$\tau_1=h\langle E\rangle^{-\frac{1}{2}}, \tag{24}$$

then an integral model for dissipation in the mixed layer, independent of viscosity and the small scales, is

$$\int_{-h-\delta}^{0}\epsilon dz=m_1\langle E\rangle^{\frac{3}{2}}, \tag{25}$$

where m_1 is a constant of proportionality. For those situations where the turbulent velocity scale $\langle E\rangle^{\frac{1}{2}}$ is proportional to the surface friction velocity u_*, Eq. (25) is equivalent to the parameterization used by Miropol'skiy (1970) and Denman (1973). Such is the case only for neutral, $\overline{bw}(0)=0$, mixed layers.

2) A limiting dissipation time scale for deeper (Ro∼1) mixed layers

In deeper boundary layers, planetary rotation turns the mean shear direction with depth and thus influences the geometrical aspects of the integral scale. This introduces a second integral time scale

$$\tau_2=f^{-1}, \tag{26}$$

the inverse of the coriolis parameter.

It is becoming increasingly clear from such studies as Arya and Wyngaard (1975) and Sundararajan (1975) that this rotational time scale plays an important role in the internal structure of the convective planetary

[3] This D is equivalent to the D^*/ρ_0 of Kraus and Turner (1967), where D^* is the total rate of dissipation per unit area.

boundary layer or mixed layer. The concern here is more with the bulk properties of the region and less with the details within the mixed layer, but it is suggested that this time scale has an important role in the overall turbulent energy budget. The mean shear profile and the turbulent energy budget are inseparable because of the link through local shear production.

Rather than to simply replace the convective scale τ_1 by the rotational scale τ_2, it is assumed that

$$(\tau_e)^{-1}=(\tau_1)^{-1}+(\tau_2)^{-1}. \tag{27}$$

This is the simplest combination of the two scales that retains the asymptotic characteristic of $\tau_e \to \tau_1$ as $hf \to 0$. This gives

$$D=\int_{-h-\delta}^{0} \epsilon dz = m_1\langle \tilde{E}\rangle^{\frac{3}{2}}+m_b fh\langle \tilde{E}\rangle \tag{28}$$

or

$$D=m_1\langle \tilde{E}\rangle^{\frac{3}{2}}\left(1+\mathrm{Ro}^{-1}\frac{m_b}{m_1}\frac{u_*}{\langle \tilde{E}\rangle^{\frac{1}{2}}}\right), \tag{28a}$$

where

$$\mathrm{Ro}=\frac{u_*}{hf} \tag{29}$$

is a Rossby number for the turbulent boundary layer.

b. Redistribution of turbulent energy

The vertical integral of the pressure redistribution term,

$$R_\alpha=\int_{-h-\delta}^{0}\overline{\frac{p}{\rho_0}\frac{\partial u_\alpha}{\partial x_\alpha}}dz, \tag{30}$$

is an important source or sink term for the individual turbulent kinetic energy budgets, even though $R_1+R_2+R_3=0$.

Following the early lead of Rotta (1951), and in agreement with the dominant term of the rational closure technique of Lumley and Khajeh-Nouri (1974), the bulk formulation is

$$R_\alpha=m_2\langle \tilde{E}\rangle^{\frac{1}{2}}(\langle \tilde{E}\rangle-3\langle \overline{u_\alpha^2}\rangle). \tag{31}$$

In addition to dimensional consistency, the concept leading to (31) is that of a "return to isotropy." In other words, the pressure-strain rate interaction tends to restore equal distribution of energy among the three components. This interaction is expected to be somewhat dependent upon stability, but this is assumed to be a higher order effect and is neglected here. The rotational redistribution terms $\Omega_\alpha\overline{uu_\alpha}$ are also assumed to be of a higher order and are neglected at this point. Their inclusion would, however, create the intriguing possibility of entrainment rate being susceptible to wind direction.

c. Shear production

The vertical integral of shear production reduces to

$$-\int_{-h}^{0}\left(\overline{uw}\frac{\partial U}{\partial z}+\overline{vw}\frac{\partial V}{\partial z}\right)dz\approx u_*^2\delta U(0), \tag{32}$$

where $\delta U(z)$ is the magnitude of the mean velocity associated with mean shear, i.e.,

$$\delta U(z)=[U^2+V^2-\langle U^2\rangle-\langle V^2\rangle]^{\frac{1}{2}}. \tag{33}$$

In this instance, the inhomogeneity of the mean velocity field cannot be neglected. An additional source/sink term is

$$\int_{-h-\delta}^{0}-\frac{\partial}{\partial z}\left[\overline{w\left(\frac{p}{\rho_0}+\frac{E}{2}\right)}\right]dz=-\left[\overline{w\left(\frac{p}{\rho_0}+\frac{E}{2}\right)}\right]_0-\left[\frac{\overline{wp}}{\rho_0}\right]_{-h-\delta}. \tag{34}$$

The surface term reflects a source attributable to breaking surface waves, and it might be modeled as being proportional to u_*^3 for a fully developed wave field. The term at $z=-h-\delta$ accounts for a possible loss due to downward-radiating internal wave energy. Stull (1975) found that this may be significant in a rapidly deepening unstable atmospheric boundary layer. The term will be neglected here.

If $\delta U(0)$ is proportional to u_*, then (32) may be combined with (34) to give net "wind-generated" rate of production[4]:

$$G=\int_{-h-\delta}^{0}-\left[\overline{uw}\frac{\partial U}{\partial z}+\overline{vw}\frac{\partial V}{\partial z}+\frac{\partial}{\partial z}\left(\frac{\overline{wp}}{\rho_0}+\frac{\overline{wE}}{2}\right)\right]dz=m_3u_*^3+\frac{(\Delta U)^2+(\Delta V)^2}{2}\frac{\partial h}{\partial t}. \tag{35}$$

The last term of (35) comes from integrating the shear production across the entraining interface (Niiler, 1975).

d. Summary of modeled equations

A final set of equations has been generated:

The extrainment buoyancy flux, from (17) is

$$-\overline{bw}(-h)=\frac{m_4\langle \overline{w^2}\rangle^{\frac{1}{2}}\langle \tilde{E}\rangle}{h}. \tag{36}$$

The budget for the horizontal components of turbulent kinetic energy comes from (35a), (31), (28) and the

[4] This G is equivalent to Kraus and Turner's G^*/ρ_0 plus the term added by Niiler.

sum of (19a) and (19b) vertically integrated, giving

$$\frac{1}{2}\frac{\partial}{\partial t}(h\overline{\langle u^2+v^2\rangle}) = m_3 u_*^3 - \frac{bw(-h)|\Delta C|^2}{2\Delta B}$$

$$-m_2(\langle E\rangle - 3\overline{\langle w^2\rangle})\langle E\rangle^{\frac{1}{2}} - \frac{2m_1}{3}\left(\langle E\rangle^{\frac{1}{2}} + \frac{m_5}{m_1}fh\right)\langle E\rangle. \quad (37)$$

The budget for the vertical component of turbulent kinetic energy comes from (31), (28) and the vertical integral of (19c), giving

$$\frac{1}{2}\frac{\partial}{\partial t}(h\overline{\langle w^2\rangle}) = \tfrac{1}{2}hbw(-h) - \tfrac{1}{2}hu_*b_* + m_2(\langle E\rangle - 3\overline{\langle w^2\rangle})\langle E\rangle^{\frac{1}{2}}$$

$$-\frac{m_1}{3}\left(\langle E\rangle^{\frac{1}{2}} + \frac{m_5}{m_1}fh\right)\langle E\rangle. \quad (38)$$

The mean buoyancy and complex mean momentum equations are

$$h\frac{\partial\langle B\rangle}{\partial t} = \overline{bw}(-h) - \overline{bw}(0) + \frac{\alpha g}{\rho_0 C_p}Q_0, \quad (20)$$

$$h\frac{\partial\langle C\rangle}{\partial t} = \overline{cw}(-h) - \overline{cw}(0) - if\langle C\rangle h. \quad (21)$$

The jump conditions relate the entrainment fluxes to the mean momentum and mean buoyancy and the rate of deepening,

$$-\overline{cw}(-h) = \Delta C\frac{\partial h}{\partial t}, \quad (14)$$

$$-\overline{bw}(-h) = \Delta B\frac{\partial h}{\partial t}. \quad (13)$$

The values of $\overline{uw}(0)$, $\overline{vw}(0)$, $\overline{bw}(0)$ and the radiation absorption $Q(z)$ are assumed to be given time-dependent variables from which are determined

$$u_*^2 = |\overline{uw}(0) + i\overline{vw}(0)|, \quad (39)$$

$$u_*b_* = -\overline{bw}(0) - \frac{\alpha g}{\rho_0 C_p}\int_{-h-\delta}^{0}\left(Q - \frac{2}{h+\delta}\int_z^0 Q\,d\lambda\right)dz. \quad (40)$$

Also assumed to be given are the mean buoyancy and momentum just below the mixed layer: $B(-h-\delta)$ and $C(-h-\delta)$. Therefore

$$\left.\begin{aligned}\Delta B &= \langle B\rangle - B(-h-\delta)\\ \Delta C &= \langle C\rangle - C(-h-\delta)\end{aligned}\right\}.$$

5. General behavior of the equations

a. Nondimensional form of the turbulent energy and entrainment equations

Using the given flux scales u_* and b_*, new dimensionless variables are defined:

$$H^* = \frac{u_*b_*h}{2m_3u_*^3}, \quad (41)$$

$$P^* = \frac{h\Delta B}{2m_3u_*^3}\frac{\partial h}{\partial t} = \frac{-h\overline{bw}(-h)}{2m_3u_*^3}, \quad (42)$$

$$E_{ii}^* = \left(\frac{m_1}{m_3}\right)^{\frac{1}{3}}\frac{\langle E\rangle}{u_*^2}, \quad (43)$$

$$E_{33}^* = \left(\frac{m_1}{m_3}\right)^{\frac{1}{3}}\frac{\overline{\langle w^2\rangle}}{u_*^2}. \quad (44)$$

The mixed layer stability parameter H^* is the ratio of the effective buoyancy flux (from surface heating and net precipitation minus evaporation) to wind-stress production. It is proportional to h/L where L is the Obukhov length. Both L and H^* may be negative should there be a positive surface buoyancy flux due to surface cooling and/or a net evaporation minus precipitation. A value of zero for H^* ($L\to\infty$) represents a neutral mixed layer. The interface stability parameter P^* is a dimensionless measure of the entrainment rate. The parameters E_{ii}^* and E_{33}^* are measures of the total turbulent kinetic energy and the vertical component of turbulent kinetic energy respectively. The values of P^* and $E_{\alpha\alpha}^*$ will depend upon the values of H^* and Ro^{-1} that are determined by the prescribed values of u_*^2 and u_*b_* together with the current value of h.

Invoking the quasi-steady-state assumption for the turbulent energy budget, the entrainment and turbulent energy equations (36), (37) and (38), become

$$P^* = \tfrac{1}{2}p_1E_{ii}^*(E_{33}^*)^{\frac{1}{2}}, \quad (45)$$

$$0 = 1 + \frac{P^*}{\mathrm{Ri}^*} - p_2(E_{ii}^* - 3E_{33}^*)(E_{ii}^*)^{\frac{1}{2}}$$

$$-\tfrac{2}{3}E_{ii}^*(E_{ii}^{*\frac{1}{2}} + p_3\,\mathrm{Ro}^{-1}), \quad (46)$$

$$0 = -H^* - P^* + p_2(E_{ii}^* - 3E_{33}^*)(E_{ii}^*)^{\frac{1}{2}}$$

$$-\tfrac{1}{3}E_{ii}^*(E_{ii}^{*\frac{1}{2}} + p_3\,\mathrm{Ro}^{-1}), \quad (47)$$

where

$$\mathrm{Ri}^* = h\Delta B/|\Delta C|^2,$$

$$p_1 = m_4/m_1, \quad (48a)$$

$$p_2 = m_2/m_1, \quad (48b)$$

$$p_3 = m_5/m_1. \quad (48c)$$

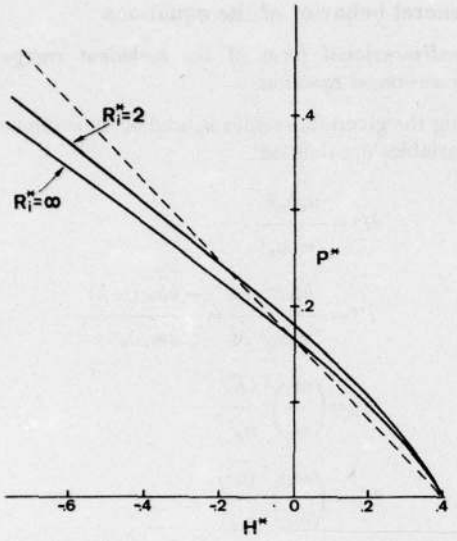

FIG. 4. Dimensionless entrainment buoyancy flux P^* versus layer stability H^* for the case of Ro$\gg$1. The dashed line is the "calibrated" solution to the Kraus-Turner prototype model.

b. Determination of the constants

Observations of changes in the vertical structure of the upper ocean together with simultaneous measurements of the surface fluxes will eventually be used to determine the validity of the closure hypotheses and to establish values for the required constants. However, approximate values will be estimated here so that solutions to the equations may be computed for a preliminary evaluation of the model.

The ratio m_2/m_1 is equivalent to $18l_1/\Lambda$, where l_1/Λ is the redistribution to dissipation length scale ratio of Mellor and Herring (1973). From boundary layer data, they find $l_1/\Lambda=0.05\pm0.01$. Hence p_2 is of order 1 and will be taken to be equal to 1 in this analysis,

$$p_2=1. \tag{49}$$

The ratio $m_4/m_1=p_1$ may be determined by considering the asymptotic case of pure convection, $H^*\to-\infty$, Ri$^*=\infty$ and Ro$=\infty$. Then (45), (46) and (47) reduce to

$$p_1=\frac{2r}{1-r}\left(\frac{E^*_{33}}{E^*_{ii}}\right)^{-\frac{1}{2}}, \tag{50}$$

$$E^*_{33}/E^*_{ii}=(3p_2+2)/(9p_2). \tag{51}$$

Eqs. (49), (50) and (51) combine to make p_1 solely dependent upon r:

$$p_1=18r/[5(1-r)].$$

If, again for the sake of a preliminary solution, p_1 is also taken to be unity,

$$p_1=1, \tag{52}$$

this corresponds to $r=5/23$, which is within the expected range of 0.2 ± 0.1. P^* may now be solved as a function of H^* and Ri*. Fig. 4 shows $P^*(H^*)$ for Ri$^*=2$ and for Ri$^*=\infty$. There is an obvious increase in rate of entrainment P^* with decreasing layer stability H^*. The important point is that the non-zero curvature, $\partial^2P^*/\partial H^{*2}$, means that the percentage of turbulent energy going to entrainment changes with H^*.

In the retreat mode ($P^*=0$), H^* is at its maximum value (0.4 in the case of $p_1=p_2=1$). The value of P^* goes to zero as the ratio of vertical to horizontal turbulent energy (illustrated in Fig. 5) vanishes. It is not expected that E^*_{33} need be identically zero in the event of retreat, but the large value of $|\partial P^*/\partial H^*|$ in the vicinity of $H^*_{\max}$ minimizes the importance of this detail. Total turbulent energy E^*_{ii} is still substantial at $H^*=H^*_{\max}$ so dissipation remains significant in the retreat mode. In the event of retreat, the mixed layer depth $h=h_r$ is no longer determined by (45), but by $H^*=H^*_{\max}$ or

$$h_r=\frac{2m_3u_*^2}{u_*b_*}H^*_{\max}. \tag{53}$$

Fig. 4 also indicates that entrainment shear production has only a small effect on entrainment rate if Ri$^*\gtrsim2$. This effect will only be important during a fraction of one inertial period following a strong increase in wind stress, especially after a period of strong surface heating and minimal mixed layer depth. In such a case, a mean flow instability as suggested by Pollard *et al.* (1973) is consistent with the prediction from (10) that the ratio δ/h adjusts to keep Rδ constant. That is, this instability could take place as δ approaches h in value.

The one remaining constant needed to complete the shallow-layer model is m_3. This may be determined

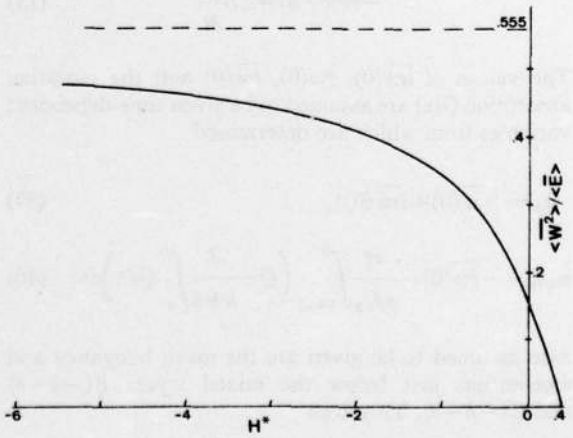

FIG. 5. Ratio of vertical turbulent kinetic energy to total turbulent kinetic energy for Ri$^*\gg$1 and Ro$\gg$1. The unstable limit ($H^*\to-\infty$) is 0.555.

from the Kato and Phillips (1969) laboratory results,

$$h\Delta B\frac{\partial h}{\partial t}(b_*=0)=2.5u_*^3, \tag{54}$$

together with $P^*(H^*=0)$ from Fig. 4,

$$P^*(H^*=0)=\frac{h\Delta B}{2m_3u_*^3}\frac{\partial h}{\partial t}(b_*=0)=0.165,$$

giving

$$m_3=1.25/P^*(H^*=0)=7.6. \tag{55}$$

A check on this value comes from (32). Eqs. (32) and (35), with $\mathrm{Ri}^*>2$, give

$$m_3=\delta U(0)/u_*. \tag{56}$$

Therefore, a value of $m_3=7.6$ is quite reasonable.

c. General solution—including dissipation enhancement

The general solution to P^* is largely a function of only two variables, H^* and Ro^{-1} if $\mathrm{Ri}^*\gtrsim 2$. This solution, from Garwood (1976), is given in Fig. 6. It is the result of the simultaneous solutions of (45), (46) and (47). The earlier solution (Fig. 4) is represented by the limiting case, $P^*(\mathrm{Ro}^{-1}=0)$. In examining Fig. 6, $Z^*=p_3\mathrm{Ro}^{-1}$ may be regarded as the nondimensional mixed-layer depth and H^* may be considered a measure of stability. Two new features appear in the general solution. First, the rate of entrainment decreases with increased Z^*. Second, in the retreat mode ($P^*=0$), $H^*_{\max}$ is not a constant but is a function of layer depth, rotation and wind stress. In particular, a neutral steady state, $P^*=0$ for $H^*=0$, is predicted for a sufficiently large value of Z^*. However, starting with $h\ll u_*/f$, neutral steady state would be approached only after a relatively long time. This is not likely to be achieved in geophysical flows, except perhaps by the atmospheric boundary layer during the polar winter (Businger and Arya, 1974).

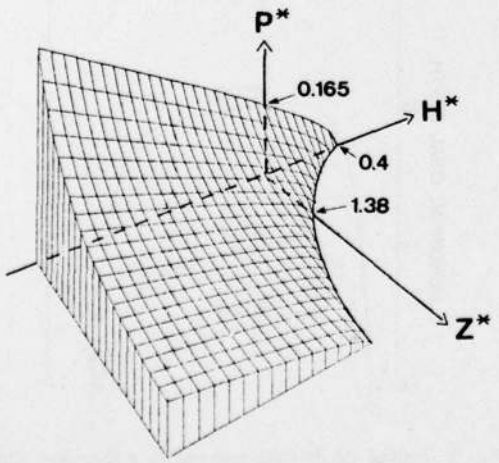

FIG. 6. General solution to the entrainment and turbulent kinetic energy equations (45), (46) and (47), if $\mathrm{Ri}^*\gg 1$ and $p_1=p_2=1$.

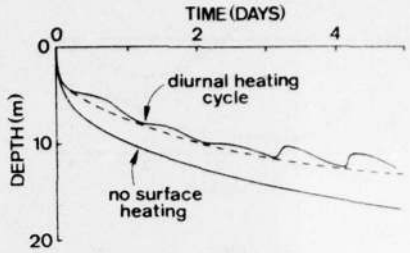

FIG. 7. Mixed layer depth versus time for two hypothetical cases having constant wind stress and an initial linear stratification. The case with a diurnal heating cycle exhibits a modulation of the longer term rate of deepening, as predicted by (57).

6. Specific differences in comparison to earlier models

a. Nonlinearity in $P^*(H^*)$ in deepening mixed layers

This nonlinearity is present with or without rotation. Therefore it is sufficient to examine the simpler case with $\mathrm{Ro}\gg 1$ (Fig. 4) to demonstrate this effect. If H^* is perturbed by a fluctuating surface buoyancy flux such as that associated with the diurnal-period heating cycle, then the mean P^* over a complete cycle will be less than P^* for the mean H^*, i.e.,

$$\overline{P^*(H^*)}\lesssim P^*(\overline{H^*}). \tag{57}$$

Fig. 7 demonstrates the consequence of this phenomenon over the course of a few days. This nonlinearity will result in the modulation of the long-term trend by shorter period fluctuations in stability, particularly those of the diurnal cycle.

b. Cyclical steady state

For the sake of studying the relative response of the mixed layer, all cycles will be assumed to be repetitive (in steady state). A sinusoidal surface buoyancy flux[5] and a constant wind stress are used to drive the model, i.e., $|\overline{cw}(0)|=u_*^2=\text{constant}$ and $-\overline{bw}(0)=|u_*b_*|i\times\exp(-i\omega t)$. In other words, in this hypothetical case, $\overline{bw}(0)$ is assumed to have no mean components. The period $2\pi/\omega$ is not specified, but the results will be particularly relevant to the annual heating/cooling cycle. The diurnal cycle is not as likely to be in a steady state, but the result will also approximate that response.

[5] The effective surface buoyancy flux is, for the sake of convenience, assumed here to include the solar radiation component (as if all shortwave radiation were absorbed at the immediate surface).

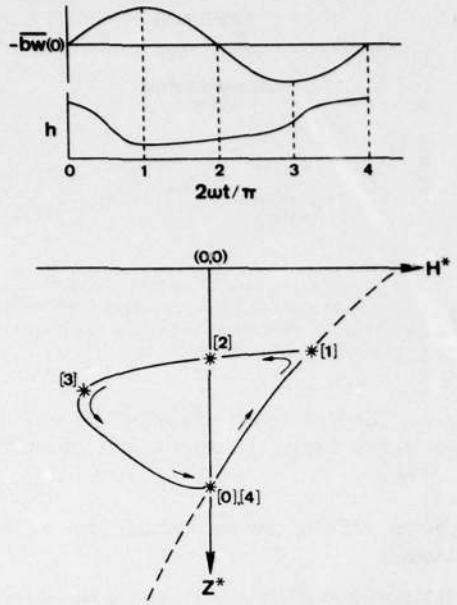

FIG. 8. The cyclical response of $h(t)$ and the corresponding closed loop in the (Z^*, H^*) plane due to an imposed periodic surface buoyancy flux $-\overline{bw}(0)$.

Cyclical steady state is depicted by Fig. 8. This shows the locus of coordinates (Z^*,H^*) as the effective surface buoyancy flux progresses through a heating $[\overline{bw}(0)<0]$ and then a cooling $[\overline{bw}(0)>0]$ phase. The initial [0] and final [4] points coincide at the point for the neutral steady state. On an annual basis, this would also correspond to the vernal equinox. Between [0] and [1] the buoyancy flux is directed downward $(H^*>0)$ and is increasing, causing the mixed layer to retreat to its minimum depth at [1]. Between [1] and [2] there is active entrainment, $\partial h/\partial t>0$, but the rate of deepening is very slow because of continued downward surface buoyancy flux. In spite of this downward surface heat flux, the sea surface temperature will begin to drop as soon as entrainment heat flux becomes dominant, i.e., $-\overline{\theta w}(-h)>-\overline{\theta w}(0)$. This will occur prior to the autumnal equinox [2]. Because of the large seasonal buoyancy gradient created during the summer when the heat added through the surface was not mixed deeply, h does not increase rapidly until after the surface heat flux maximum at [3]. Of course, autumn storms (with greatly increased u_*^3 and enhanced evaporation) could more quickly overcome this buoyancy gradient and accelerate the rate of deepening. Any particular oceanic region has neither a constant wind stress nor a perfectly sinusoidal buoyancy flux. Any mean (over one year) buoyancy flux can only be accounted for by including advection, which has not been done here. However, the purpose here has been to show that a one-dimensional mixed layer model can explain the observed cyclical steady state. The inclusion of advection and more realistic surface forcing would alter to some extent the shape and relative position of the predicted *closed* locus in the (Z^*,H^*) plane.

The relative importance of the rotational and surface buoyancy flux scales needs to be examined. The magnitude of the mixed layer response is found to be a function of the ratio of the rotational length scale (u_*/f) to the buoyancy flux scale (u_*^2/b_*), i.e.,

$$B^*=\frac{|u_*b_*|}{fu_*^2}. \tag{58}$$

Fig. 9 shows the cycle of $h(t)$, nondimensionalized on u_*/f as a function of B^*.

For large B^*, which is typical of the annual cycle in temperate oceanic regions, the shallow mixed layer depth at $\omega t=\pi/2$ is attributable to the strong influence of the buoyant damping corresponding to a small positive Obukhov length scale. A more realistic, nonconstant u_* would influence the time for the occurrence of this minimum layer depth. In addition to the change in the range of h with B^*, there is an effect upon the shape of the function $h(t)$. For the case of weak heating and cooling, the variation in h is almost in phase with $\overline{bw}(0)$. In the (Z^*, H^*) plane, the locus of the cycle is small and elongated. For increasingly larger B^*, the heat and therefore buoyancy is stored during the "summer" at an increasingly shallower depth (in comparison to $h_{max}\sim u_*/f$). This creates a hysteresis effect by retarding the subsequent rate of deepening. This phase lag in the heat storage naturally has important implications for the interaction with the atmosphere for all surface flux time scales, from one day to periods of climatological importance.

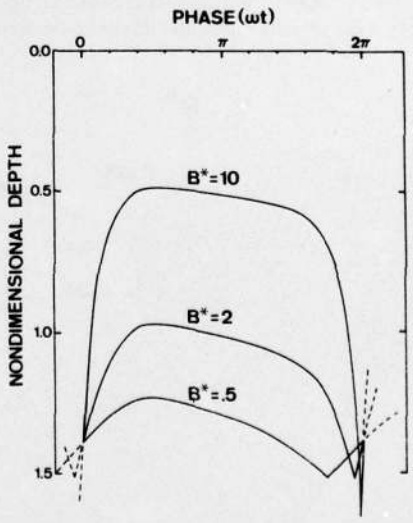

FIG. 9. Cyclical steady-state response to a sinusoidal surface buoyancy flux and a constant wind stress. Mixed layer depth is nondimensionalized on u_*/f and $B^*=|u_*b_*|/(fu_*^2)$ is a measure of the strength of the annual heating/cooling cycle.

7. A theoretical framework for model comparison and testing

Fig. 6, in which the solution for entrainment rate is depicted as a function of stability (H^*) and a second parameter Z^* ($=p_3\mathrm{Ro}^{-1}$ in the present formulation), poses a framework for model intercomparison. Fig. 10 shows illustrations of the P^* surface as predicted by three representative models.

Fig. 10a is that for the Kraus-Turner (KT) type of model. This is representative of all models (including those of Miropol'skiy, Denman and Niiler) for which shear production G is parameterized as being proportional to u_*^3, and net dissipation D is a fixed fraction of G, giving

$$P^*_{\mathrm{KT}}=c_1-c_2H^*. \tag{59}$$

In this case there is no dissipation enhancement with increased layer depth or rotation, as measured by the second variable Z^*.

Fig. 10b is for the Elsberry *et al.* (EFT) model in which $D\propto 1-\exp(-Z^*)$. As in the KT model, P^* depends linearly upon H^*, but the rate of deepening is checked with increased $Z^*=h/Z$:

$$P^*_{\mathrm{EFT}}=c_1\exp(-Z^*)-c_2H^*. \tag{60}$$

This dissipation enhancement, however, is still insufficient to predict a cyclic steady state because the locus of $P^*=0$ fails to cross the $H^*=0$ line.

Fig. 10c is for the model of Kim (1976) having a constant background dissipation ϵ_0 in addition to the fixed fraction of shear production, giving

$$P^*_{\mathrm{K}}=c_1-c_3Z^*-c_2H^*. \tag{61}$$

Notice that (61) predicts a possible steady state, both neutral and cyclical, because the $P^*=0$ locus crosses the $H^*=0$ line at $Z^*=c_1/c_3$. Kim's background dissipation is not necessarily as strong at that of EFT for small Z^*, but this parameterization denotes a stronger net dissipation with increasingly larger values of Z^*.

If the dissipation enhancement effects of EFT, Kim and Garwood are assumed to be physically equivalent and $Z^*=p_3\mathrm{Ro}^{-1}$, then Elsberry's Z and Kim's ϵ_0 are both related to planetary rotation, i.e.,

$$Z\propto u_*/f, \tag{62}$$

$$\epsilon_0\propto fu_*^2. \tag{63}$$

Resnyanskiy (1975) also suggests that this second length scale Z should be proportional to u_*/f. It is an interesting development to find that present-day workers are returning to the rotational length scale originally proposed by Rossby and Montgomery (1935).

The framework $P^*(Z^*, H^*)$ is also applicable to data analysis. An empirical determination of the P^* surface as a function of Z^* and H^* is needed to test and further improve the one-dimensional model. Actually accomplishing such an empirical fit is difficult because it requires identifying the true depth of the turbulent boundary layer. This may only occasionally coincide with the apparent $h(t)$ because the diurnal variation in stability will give rise to a diurnal retreat and deepening cycle, not easily discernable in temperature profiles. Nevertheless, this information is needed to adequately test a model. Any particular mixed layer model may be calibrated to predict the apparent $h(t)$ at a suitable site as long as the variations in H^* and Z^* are small, but such a model may be of little use under widely varying conditions.

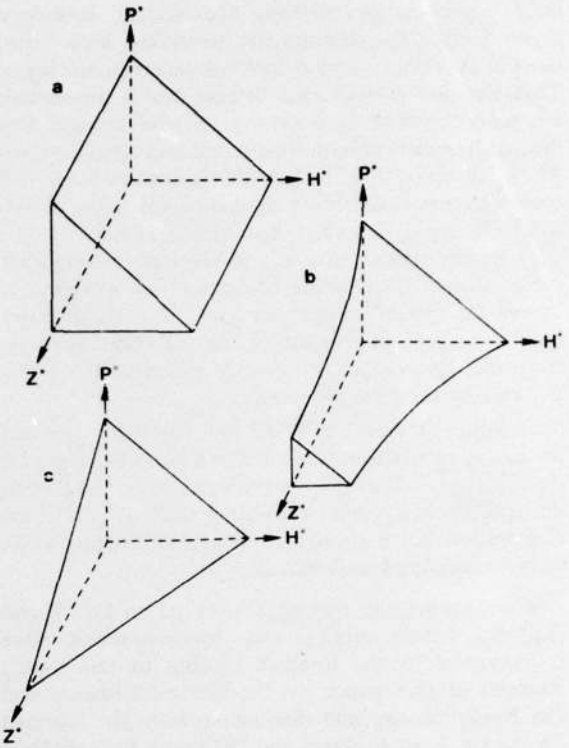

FIG. 10. Solutions to the entrainment function P^* in the (H^*, Z^*) plane for the models of (a) Kraus and Turner (1967), (b) Elsberry *et al.* (1976) and (c) Kim (1976). Compare these with Fig. 6.

8. Conclusions

This new model for the ocean mixed layer suggests answers to the questions raised earlier concerning the general applicability of bulk models based upon the turbulent energy budget:

1)Planetary rotation is assumed to influence the dissipation time scale for the turbulence. This enhances dissipation for deeper mixed layers and enables a cyclical steady state on an annual basis.

2) The rate of entrainment (P^*) for the stable regime, $H^*>0$, is not accurately reflected by a linear extrapolation of the $H^*\leqslant 0$ situations. This is particu-

larly important in modeling the oceanic boundary layer. Unlike the atmospheric boundary layer case, most of the solar radiation does not penetrate the layer. Therefore downward turbulent heat flux in the oceanic boundary layer is as important as the upward flux during the course of both the diurnal and annual cycles. The nonlinearity of $P^*(H^*)$, which is greatest for $H^*>0$ results in a modulation of the long-term trend of $h(t)$ by the diurnal component of surface heat flux.

3) In this model, buoyant production is somewhat more efficient than shear production as a source of energy for vertical mixing because of its unique effect on the vertical component of the turbulent velocity. However, this efficiency is much less than the 100% denoted by the prototype model.

Finally, a framework, $P^*(Z^*, H^*)$ has been suggested for model comparison. This is also a potential basis for data analysis and experiment design. While the models do have didactic value, knowledge of $P^*(Z^*, H^*)$ from observations alone would be sufficient for the prediction of layer deepening and retreat.

Acknowledgments. Special thanks go to Dr. David Halpern, whose advice and encouragement were instrumental in the research leading to this paper. Reviews of this paper by Dr. Russell Elsberry and Dr. Robert Haney and discussions with Mr. Norman Camp, Dr. Joost Businger and Dr. Frank Badgley have been most useful in bringing this work into its present form. This study was supported by NOAA's Environmental Research Laboratories and by NOAA's GATE Office, and this support is gratefully acknowledged. Additional support for the preparation of the manuscript was provided by the Office of Naval Research under ONR Contract N000147TWRT0042-NR083-275-5.

REFERENCES

Arya, S. P. S., and J. C. Wyngaard, 1975: Effect of baroclinicity on wind profiles and the geostrophic drag law for the convective planetary boundary layer. *J. Atmos. Sci.*, **32**, 767–778.

Benjamin, T. B., 1963: The threefold classification of unstable disturbances in flexible surfaces bounding inviscid flows. *J. Fluid Mech.*, **16**, 435–450.

Bradshaw, P., 1972: The understanding and prediction of turbulent flow. *Aeronaut. J.*, **76**, 403–418.

Businger, J. A., and S. P. S. Arya, 1974: Height of the mixed layer in the stably stratified planetary boundary layer. *Advances in Geophysics*, Vol. 18A, Academic Press, 73–92.

Camp, N. T., 1976: The role of strong atmospheric forcing events in the modification of the upper ocean thermal structure during the cooling season. Ph.D. thesis, Naval Postgraduate School.

Csanady, G. T., 1974: Equilibrium theory of the planetary boundary layer with an inversion lid. *Bound. Layer Meteor.*, **6**, 63–79.

Denman, K. L., 1973: A time-dependent model of the upper ocean. *J. Phys. Oceanogr.*, **3**, 173–184.

Elsberry, R. L., T. S. Fraim and R. N. Trapnell, 1976: A mixed layer model of the oceanic thermal response to hurricanes. *J. Geophys. Res.*, **81**, 1153–1162.

Garwood, R. W., 1976: A general model of the ocean mixed layer using a two-component turbulent kinetic energy budget with mean turbulent field closure. Ph.D. thesis, University of Washington, (NOAA Tech. Rep. ERL 384-PMEL 27).

Geisler, J. E., and E. B. Kraus, 1969: The well-mixed Ekman boundary layer. *Deep Sea Res.*, **16**, Suppl., 73–84.

Gill, A. E., and J. S. Turner, 1976: A comparison of seasonal thermocline models with observation. *Deep Sea Res.*, **23**, 391–401.

Halpern, D., 1974: Observations of the deepening of the wind-mixed layer in the northeast Pacific Ocean. *J. Phys. Oceanogr.*, **4**, 454–466.

Kato, H., and O. M. Phillips, 1969: On the penetration of a turbulent layer into stratified fluid. *J. Fluid Mech.*, **37**, 643–655.

Kim, J., 1976: A generalized bulk model of the oceanic mixed layer. *J. Phys. Oceanogr.*, **6**, 686–695.

Kitaigorodsky, S. A., 1960: On the computation of the thickness of the wind-mixing layer in the ocean. *Bull. Acad. Sci. U.S.S.R. Geophys. Ser.*, **3**, 284–287.

Kraus, E. B., and J. S. Turner, 1967: A one-dimensional model of the seasonal thermocline, part II. *Tellus*, **19**, 98–105.

Lamb, H. L., 1932: *Hydrodynamics*. Dover, 738 pp.

Lumley, J. L., and B. Khajeh-Nouri, 1974: Computational modeling of turbulent transport. *Advances in Geophysics*, Vol. 18A, Academic Press, 169–192.

Mellor, G. L., and P. A. Durbin, 1975: The structure and dynamics of the ocean surface mixed layer. *J. Phys. Oceanogr.*, **5**, 718–728.

——, and H. J. Herring, 1973: A survey of the mean turbulent field closure models. *AIAA J.*, **11**, 590–599.

Miropol'skiy, Yn. A., 1970: Nonstationary model of the wind-convection mixing layer in the ocean. *Izv. Atmos. Oceanic Phys.*, **6**, 1284–1294.

Moore, J. M., and R. R. Long, 1971: An experimental investigation of turbulent stratified shearing flow. *J. Fluid Mech.*, **49**, 635–655.

Niiler, P. P., 1975: Deepening of the wind-mixed layer. *J. Mar. Res.*, **33**, 405–422.

Pollard, R. T., P. B. Rhines and R. Thompson, 1973: The deepening of the wind-mixed layer. *Geophys. Fluid Dyn.*, **3**, 381–404.

Resnyanskiy, Y. D., 1975: Parameterization of the integral turbulent energy dissipation in the upper quasihomogeneous layer of the ocean. *Izv. Atmos. Oceanic Phys.*, **11**, 726–733.

Rossby, C. G., and R. B. Montgomery, 1935: The layer of frictional influence in wind and ocean currents. *Pap. Phys. Oceanogr. Meteor.*, **3**, No. 3, 101 pp.

Rotta, J. C., 1951: Statistiche Theorie nichthomogener Turbulenz. *Z. Phys.*, **129**, 547–572.

Stull, R. B., 1975: Temperature inversions capping atmospheric boundary layers. Ph.D. thesis, University of Washington.

Sundararajan, A., 1975: Significance of the neutral height scale for the convective, barotropic planetary boundary layer. *J. Atmos. Sci.*, **32**, 2285–2287.

Tennekes, H., 1973: A model for the dynamics of the inversion above a convective boundary layer. *J. Atmos. Sci.*, **30**, 558–567.

——, and J. L. Lumley, 1972: *A First Course in Turbulence*. The MIT Press, 300 pp.